

SLAC-PUB-7555
May 1997

CONF-970503-279

Linac Design for the LCLS Project at SLAC*

V.K. Bharadwaj, K. Bane, J. Clendenin, P. Emma, J.C. Sheppard, M.D. Woodley
Stanford Linear Accelerator Center, Stanford University, Stanford, CA 94309

RECEIVED

JUL 17 1997

OSTI

Abstract

The Linac Coherent Light Source (LCLS) at SLAC is being designed to produce intense, coherent 0.15-nm x-rays. These x-rays will be produced by a single pass of a 15-GeV bunched electron beam through a long undulator. Nominally, the bunches have a charge of 1 nC, normalized transverse emittances of less than 1.5π mm-mr and an rms bunch length of 20 μm . The electron beam will be produced using the last third of the SLAC 3-km linac in a manner compatible with simultaneous operation of the remainder of the linac for PEP-II. The linac design necessary to produce an electron beam with the required brightness for LCLS is discussed, and the specific linac modifications are described.

*Contributed to the 1997 Particle Accelerator Conference
Vancouver, B.C., Canada, May 12-16, 1997*

MASTER

DISCLAIMER

This report was prepared as an account of work sponsored by an agency of the United States Government. Neither the United States Government nor any agency thereof, nor any of their employees, makes any warranty, express or implied, or assumes any legal liability or responsibility for the accuracy, completeness, or usefulness of any information, apparatus, product, or process disclosed, or represents that its use would not infringe privately owned rights. Reference herein to any specific commercial product, process, or service by trade name, trademark, manufacturer, or otherwise does not necessarily constitute or imply its endorsement, recommendation, or favoring by the United States Government or any agency thereof. The views and opinions of authors expressed herein do not necessarily state or reflect those of the United States Government or any agency thereof.

DISTRIBUTION OF THIS DOCUMENT IS UNLIMITED

* Work supported by Department of Energy contract DE-AC03-76SF00515.

LINAC DESIGN FOR THE LCLS PROJECT AT SLAC*

V.K. Bharadwaj, K. Bane, J. Clendenin, P. Emma, J.C. Sheppard, M.D. Woodley
Stanford Linear Accelerator Center, Stanford, California 94309

Abstract

The Linac Coherent Light Source (LCLS) at SLAC is being designed to produce intense, coherent 0.15-nm x-rays. These x-rays will be produced by a single pass of a 15-GeV bunched electron beam through a long undulator. Nominally, the bunches have a charge of 1 nC, normalized transverse emittances of less than $1.5\pi\text{ mm-mm}$ and an rms bunch length of 20 μm . The electron beam will be produced using the last third of the SLAC 3-km linac in a manner compatible with simultaneous operation of the remainder of the linac for PEP-II. The linac design necessary to produce an electron beam with the required brightness for LCLS is discussed, and the specific linac modifications are described.

1. INTRODUCTION

The proposed LCLS [1,2] project has undergone a significant design revision in the last year. The LCLS, a 0.15-nm x-ray source, requires an extremely high quality electron beam. This beam must simultaneously have peak beam current in excess of 3.5 kA, transverse beam emittances of order $1\pi\text{ mm-mm}$, energies up to 15 GeV and bunch lengths of 20 μm . Fortunately 15 GeV of linac accelerator will become available at SLAC when the PEP-II Asymmetric B-Factory [3], which uses only the first two-thirds of the existing linac, becomes fully operational in the next few years. This 15 GeV linac with its existing infrastructure, combined with some modest modifications, makes LCLS a feasible and cost effective project.

Figure 1 shows a schematic of the LCLS linac. A new RF Gun and associated Linac-0 (L0) generates a 1-nC, $1\pi\text{ mm-mm}$ beam [4]. This beam is injected onto the existing SLAC linac axis using a dogleg inflector, DL1. The beam

DL2) to the LCLS undulator. The L2 and L3 linac hardware is essentially unchanged in the LCLS design. The RF Gun, L0, DL1, BC1, BC2 and DL2 are new installations, although existing components are used where possible. Table I lists the major accelerator parameters for the various sections of the LCLS linac.

Table I. LCLS Linac Parameters.

Parameter	L0	L1	L2	L3
Initial energy (GeV)	0.007	0.150	0.280	6.0
Final energy (GeV)	0.150	0.280	6.0	5-17
Linac length (m)	12	9	420	523
Initial sector #	20-3	20-5b	20-7	25-4
RF phase (deg)	variable	40	29	0
$\beta_{x,y}$ min/max (m)	—	2/10	10/45	35/65
Phase advance/cell (deg)	—	75	70	30
Initial $\Delta E/E$ (% rms)	0.1	0.2	2.3	1.1
Final $\Delta E/E$ (% rms)	0.2	2.3	1.1	<0.1
Bunch length (μm , rms)	~1000	1000	390	20

2. LATTICE DESIGN

The four main considerations in the optics design of the LCLS linac are to 1) minimize transverse emittance dilution due to misalignments, 2) effect the final bunch compression, 3) allow for the precise measurement of beam parameters, and 4) transport the beam to the LCLS undulator. TRANSPORT and LIAR [5] are the two main simulation tools used in the optics design.

L0 is a new 150 MeV accelerator which consists of four 3-meter s-band accelerating sections displaced 1 meter horizontally from the existing SLAC linac. Its beam dynamics, and hence its design, are dominated by space charge. It is followed by a matching section, diagnostic region and dogleg, DL1, which injects the beam into L1.

L1 is a 130 MeV linac consisting of three existing 3-meter sections. By accelerating the beam off-crest, an input energy-z correlation for BC1 is generated. Given the long bunch length and large energy spread in L1, both dispersion and transverse wakefields are sources of potential emittance growth. The LIAR code is used to study the effects of misaligned components (BPMs, quadrupoles and accelerating structures). By adding a quadrupole/BPM/steering package between each accelerating section, a lattice design with a phase advance of 75°/cell was found to keep the transverse emittance growth to less than 10%, even for very pessimistic misalignment tolerances of 300 μm . Figure 2 shows the lattice functions of L1, BC1 and their associated emittance and energy diagnostic section.

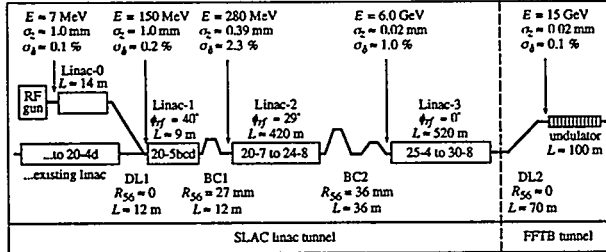


Figure 1. LCLS Linac Schematic.

is further accelerated using Linac-1, Linac-2 and Linac-3 (L1, L2, L3) and compressed in two magnetic chicanes, BC1 and BC2. The beam is then transported (beamline

* Work supported by Department of Energy contract DE-AC03-76SF00515

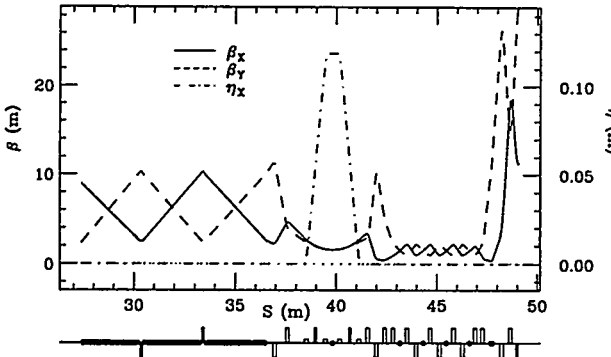


Figure 2. L1 and BC1 Lattice. The small circles on the magnet schematic at the bottom of the plot are wire scanners, four for emittance diagnostics and one for energy measurement.

L2 accelerates the beam to 6 GeV and generates an input energy-z correlation for BC2. In L2 the bunches have 1-2% energy spread, and the 400 μm RMS bunch length is still relatively long. This makes L2 very sensitive to component misalignments. In fact even with an optimized lattice, LIAR simulations still give an unacceptable factor of two transverse emittance growth due to realistic component misalignments. However, SLC experience has shown that this emittance growth can be empirically controlled using "emittance-bumps"[6]. Figure 3 shows LIAR simulation results of such bumps for a 70°/cell phase advance lattice. For 300- μm structure misalignments and 150- μm BPM and quadrupole misalignments, the transverse emittance growth is reduced from 80% to less than 10% (average of 100 seeds).

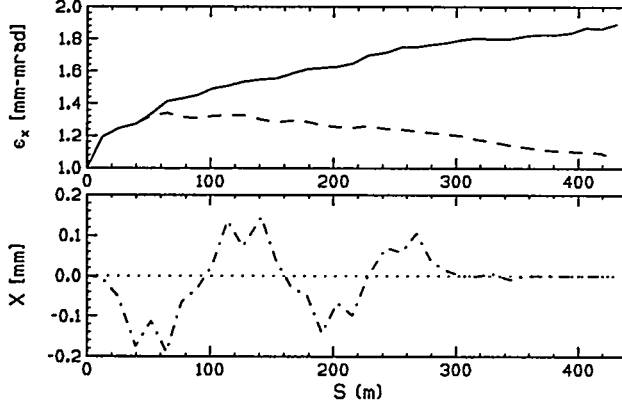


Figure 3. Emittance Bumps in L2. The upper plot shows emittance dilution without (solid) and with (dashed) emittance bumps. The lower plot shows a typical horizontal orbit distortion due to the bump.

L3 accelerates the beam to a maximum energy of 15 GeV. The bunch is too short to use rf phasing to minimize the energy spread, but fortunately the very strong longitudinal wakefield generated by the 20- μm bunch reduces the 1.1% energy spread exiting BC2 to <0.1% (<0.02% incoherent energy spread) at the undulator. The short bunch effectively eliminates transverse wake effects and the dominant emittance

dilution mechanism is due to momentum dispersion generated by quadrupole and BPM misalignments. Simulations show that a weak lattice, with a phase advance of 30°/cell and the nominal SLC quadrupole spacing, reduces the expected emittance growth to less than 10% for component misalignments as large as 300 μm . The LCLS specifications require 5-15 GeV range of electron energies. This is generated in L3 by varying the number of s-band accelerating sections used and by backphasing sections to reduce the final energy.

DL2 transports beam to the undulator, located in the existing FFTB tunnel. Figure 4 shows lattice functions for this beamline. An emittance diagnostic section is also built into the beamline. A four dipole dogleg inflector displaces the beamline 0.9 m horizontally which allows for energy analysis and a stabilizing feedback system.

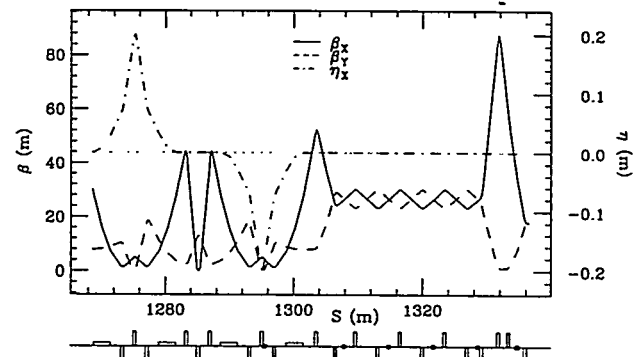


Figure 4. DL2 Beam Transport Line. Note the wire scanners for beam emittance and energy measurement in the magnet schematic.

3. BUNCH COMPRESSION

The LCLS requires peak beam currents in excess of 3.5 kA. Present electron gun technology cannot produce this current, so a series of magnetic chicane bunch compressors is used to reduce the bunch length thereby increasing the beam current. For 1 nC of accelerated charge a bunch length of 20 μm RMS is required. This corresponds to a large compression ratio of 50 for the 1-mm bunch generated by the RF photoinjector.

In designing the LCLS bunch compression scheme, care is taken to minimize non-linear effects arising from longitudinal wakefields, rf curvature and second order momentum compaction, and the sensitivity to phase and charge variations at the gun. Synchrotron radiation effects, both incoherent (ISR) and coherent (CSR), define the minimum chicane length.

Because of the large compression ratio, the LCLS accelerator has two bunch compressors, BC1 and BC2. In addition to making the magnetic chicane design easier, the two-compressor scheme allows for partial cancellation of jitter arising from gun phase and intensity variations. This cancellation seems to work best for gaussian bunch distributions out of the gun. In addition the beam is partially compressed at a low energy in BC1, and this

mitigates emittance dilution due to component misalignment at low energies.

BC1 is a simple four magnet chicane which compresses the bunch from 1 mm to 390 μm at 280 MeV. This compression ratio optimizes the cancellation of the L2 wakefield and the RF curvature and T_{566} nonlinearities of L1/BC1. BC2 has a more complicated design driven mainly by the need to minimize CSR effects due to the extremely small bunch length and strong bends. Because the energy spread generated by CSR is coherent, two consecutive chicanes of unequal strengths with a $-I$ horizontal transfer matrix between chicane centers can be tuned to cancel [7] the longitudinal to transverse coupling as shown in Figure 5.

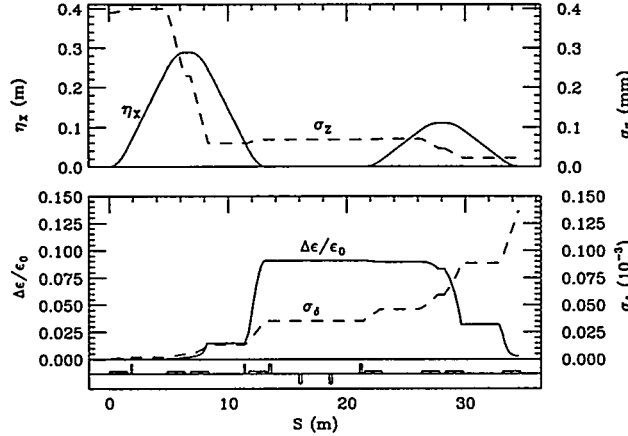


Figure 5. BC2 Double Chicane. The upper plot shows the horizontal dispersion (solid) and the bunch length (dashed) along BC2. The lower plot shows the CSR emittance growth (solid) and energy spread (dashed).

The output bunch length of BC2 is adjustable and can be tuned, along with the rf phase of L2 to compensate for the uncertainty in the magnitude of the L3 wake that sets the final energy spread. Simulations show that a 50% uncertainty can be compensated. Table II lists important BC1 and BC2 parameters. Figure 6 shows the longitudinal phase space at the input to the LCLS undulator.

4. DIAGNOSTICS AND TUNING

The design LCLS beam specifications are especially demanding. The LCLS accelerator naturally breaks down into four logical sections (RF-Gun-L0-DL1, L1-BC1, L2-BC2, L3-DL2). The diagnostic design criterion ensures that there are sufficient measurement devices so that the beam properties out of each accelerator section can be measured well and each section can be tuned to design.

The LCLS accelerator has the standard complement of BPMs, toroids, screens and beam scrapers, etc. Beam dumps are installed such that each accelerator section can be individually tuned before beam is sent to the next section and finally onto the LCLS undulator. Emittance measurement is done using a four wire scanner station. A

lattice with wires spaced by 45° of phase advance with equal beam sizes at each wire is optimum for emittance diagnostics. One such emittance measurement station is placed after each LCLS section. Additional wire scanners are placed in high dispersion points in DL1, BC1, BC2 and DL2 for energy and energy spread diagnostics.

The short LCLS bunches present a measurement challenge. Detectors using transition radiation and CSR are being designed and zero-phasing L3 can also be used to measure the absolute bunch length.

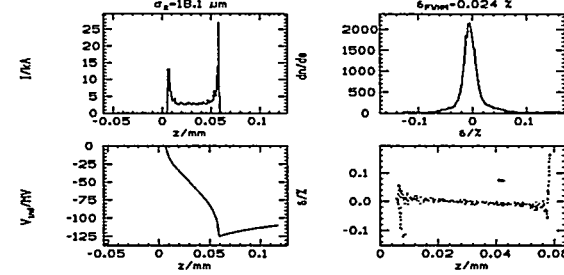


Figure 6. Longitudinal Bunch Distributions at 15 GeV. The plot shows z-distribution (top left), energy distribution (top right), longitudinal wakefield (bottom left) and energy-z correlation (bottom right).

Table II. Bunch Compressor Parameters.

Parameter	BC1	BC2
Beam energy (GeV)	0.28	6.0
Initial bunch Length (μm)	1000	390
Final bunch Length (μm)	390	20
Energy spread (%)	2.3	1.1
Momentum compaction (mm)	27.0	35.5
2nd. order mom. comp. (mm)	-40.5	-53.5
Total length (m)	2.8	34.5
Bend angle/magnet (deg)	7.1	3.4/1.3
Bend field (kG)	5.8	7.9/3.0
Max dispersion (m)	0.117	0.29/0.11
ISR emittance dilution (%)	0	1.4
CSR emittance dilution (%)	1.9	0.3

REFERENCES

- [1] M. Cornacchia, "Performance and Design Concepts of Free Electron Lasers in the X-ray Region", SLAC-PUB-7433 (1997).
- [2] K. Bane et al., "Electron Transport of a Linac Coherent Light Source (LCLS) Using the SLAC Linac", SLAC-PUB-6200 (1993).
- [3] PEP-II Asymmetric B-Factory Conceptual Design Report , SLAC-418 (1993).
- [4] A. D. Yeremian et al. , "A Proposed Injector for the LCLS Linac", these proceedings.
- [5] R. Assmann et al., "LIAR-A Computer Program for Modeling and Simulation of High Performance Linacs", SLAC/AP-103 (1996).
- [6] J. Seeman et al., "The Introduction of Trajectory Oscillations to Reduce Emittance Growth in the SLC Linac", SLAC-PUB-5705 (1992).
- [7] P. Emma et al., "Emittance Dilution Through Coherent Energy Spread Generation in Bending Systems", these proceedings.

DISCLAIMER

**Portions of this document may be illegible
in electronic image products. Images are
produced from the best available original
document.**